

# Magnetostriction and electric polarization anomalies in $\text{GdFe}_3(\text{BO}_3)_4$ single crystals at phase transitions

S.S. Krotov<sup>a,\*</sup>, A.M. Kadomtseva<sup>a</sup>, Yu.F. Popov<sup>a</sup>, G.P. Vorob'ev<sup>a</sup>, A.V. Kuvardin<sup>a</sup>,  
K.I. Kamilov<sup>a</sup>, L.N. Bezmaternykh<sup>b</sup>, E.A. Popova<sup>a</sup>

<sup>a</sup>Moscow State University, Vorob'evi Gori, Moscow 119991, Russia

<sup>b</sup>Institute of Physics SBAS, Krasnoyarsk 660036, Russia

Available online 16 November 2005

## Abstract

Our experimental and theoretical investigation was aimed at the study of different gadolinium ferroborate single-crystal properties both at spontaneous and high magnetic field-induced phase transitions.

© 2005 Elsevier B.V. All rights reserved.

PACS: 75.80.+q

Keywords: Magnetoelectric effect; Magnetostriction; Phase transitions

## 1. Introduction

Rare-earth ferroborates  $\text{RFe}_3(\text{BO}_3)_4$ , isostructural to natural mineral huntite, form when crystallized rhombohedral structure, described by trigonal space group  $R\bar{3}2(D_3^7, \# 155)$ . Particular interest to the family of  $\text{RFe}_3(\text{BO}_3)_4$  single crystals is connected with both their promising optical properties [1] and the unusual manifestation of their magnetic properties and a series of phase transitions [2,3]. Due to temperature dependence measurements of magnetic susceptibility [4] and specific heat [5] gadolinium ferroborate demonstrates while temperature decreases three consecutive phase transitions—the structural phase transition at  $T_C = 156$  K, magnetic ordering of  $\text{Fe}^{3+}$  ions at  $T_N = 38$  K and the spin-reorientation transition at  $T_R = 10$  K [4].

Our experimental and theoretical investigation was aimed at the study of different gadolinium ferroborate single-crystal properties both at spontaneous and magnetic field-induced phase transitions. Particular attention was paid to magnetic symmetry elucidation through profound

study of magnetoelectric interactions, which were studied for two magnetic field orientations— $H\parallel c$  and  $H\perp c$ .

## 2. Experiment

As far as the structural phase transition at  $T_C$  in our system is concerned we confirmed its occurrence by the measurements of thermal expansion (Fig. 1). Besides the authors of Ref. [6] discovered a singularity in the electric susceptibility behavior at  $T_C$  that in accord with our results [7] was interpreted as antiferroelectric behavior.

The longitudinal electric polarization and magnetostriction of a  $\text{GdFe}_3(\text{BO}_3)_4$  single crystal were measured in magnetic fields up to 100 kOe for  $H\parallel c$  and  $H\perp c$  in the temperature range 4.2–50 K. It was found that magnetic field below  $T_N$  induced the rearrangement of magnetic structure that was accompanied by the occurrence of the magnetoelectric effect and magnetoelastic deformations. The field dependencies of electric polarization and magnetostriction were drastically different for  $H\parallel c$  and  $H\perp c$ .

Thus, the magnetoelectric effect and magnetostriction for  $H\parallel c$  were observed only at temperatures  $T < 10$  K, vanishing in the temperature range  $10 \text{ K} < T < 38 \text{ K}$ , which are presented in Fig. 2a. This presumably indicates a

\*Corresponding author. Tel.: +7 095 939 1142; fax: +7 095 939 5907.  
E-mail address: [popov@plms.phys.msu.ru](mailto:popov@plms.phys.msu.ru) (S.S. Krotov).

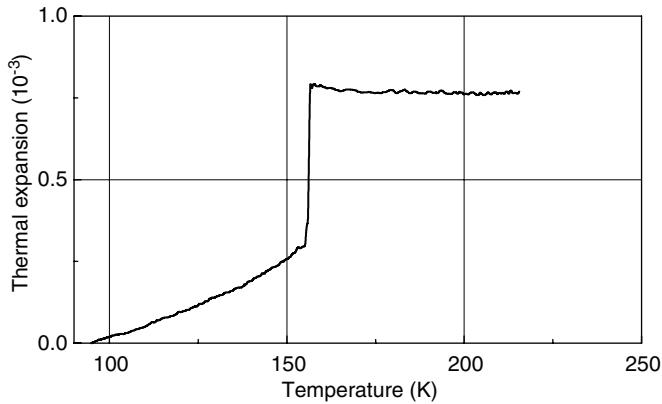


Fig. 1. Thermal expansion of  $\text{GdFe}_3(\text{BO}_3)_4$  along  $a$ -axis.

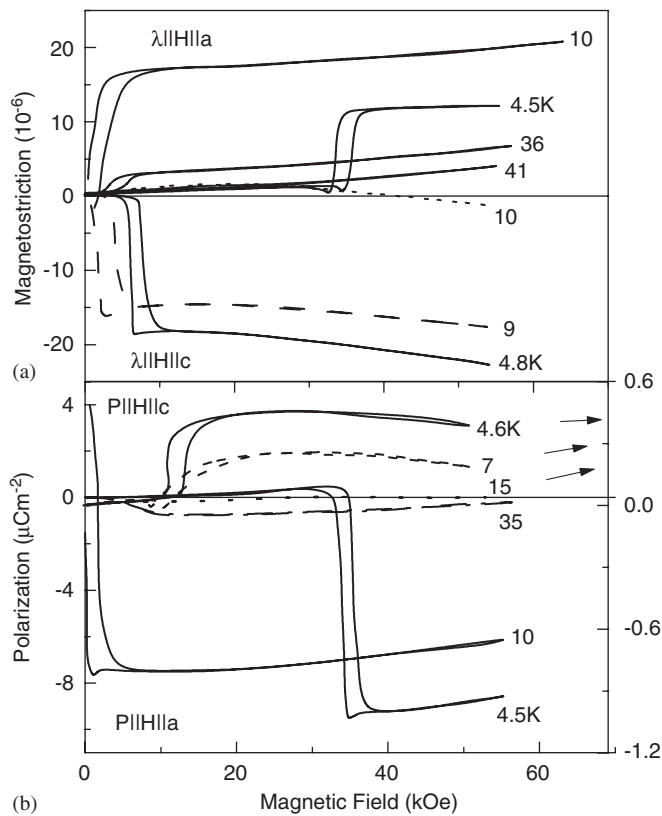


Fig. 2. Longitudinal magnetostriction (a) and electric polarization (b) of  $\text{GdFe}_3(\text{BO}_3)_4$  versus magnetic field applied along  $c$ -axis (negative magnetostriction and positive polarization) and  $a$ -axis (other curves).

symmetry change occurred near  $T_R$ . For  $H \perp c$  anomalies in the magnetoelectric effect and magnetostriction were observed for all temperatures below  $T_N$ .

It is evident that jump in the electric polarization and magnetostriction occurs in the vicinity of 5 K at a certain field  $H_C^{\text{crit}} = 8$  kOe, where a magnetic field-induced reorientation from  $c$ -axis (AF2-phase) to the easy plane (AF1-phase) was observed according to Ref. [4]. With increasing temperature the threshold fields decrease and vanish at  $T_R$ . For temperatures  $10 \text{ K} < T < 38 \text{ K}$  the longitudinal electric

polarization and magnetostriction along  $c$ -axis exhibit no anomalies and depend monotonically on the field.

The field dependencies of the longitudinal magnetostriction and electric polarization for  $H \parallel a$  are presented in Fig. 2b. It is seen that at  $T = 4.5 \text{ K}$  the electric polarization in low fields weakly depends on the magnetic field. Then it increases abruptly at  $H_a^{\text{crit}} = 37$  kOe and the polarization jump at 4.5 K for  $H \parallel a$  exceeds the polarization jump for  $H \parallel c$  by a factor 20. With increasing temperature from 4.2 K to  $T_R$  the threshold fields for the  $\text{AF1} \geq \text{AF2}$  transition strongly decrease. Starting with  $T_R$  up to  $T_N$  when the  $\text{Fe}^{3+}$  spins lie in the basal plane the electric polarization and magnetostriction increase abruptly already in a relatively weak magnetic field of  $\sim 2$  kOe and then vary monotonically when field increases.

Our results indicate that for both  $H \parallel c$  and  $H \perp c$  magnetic field orientations, magnetoelectric and magnetoelectric properties strictly correlate. It was also shown that jumps in electric polarization vector  $P$  behavior arise when the magnetic field reorients the  $\text{GdFe}_3(\text{BO}_3)_4$  single crystal from AF2 to AF1 phase. This behavior certainly points to the occurrence of ferroelectric properties in this crystal.

### 3. Theory and discussions

We remind that the unit cell of  $\text{RFe}_3(\text{BO}_3)_4$  system in rhombohedral coordinates comprises one  $\text{R}^{3+}$  ion and three  $\text{Fe}^{3+}$  ions. If the solid diagonals of elementary rhombohedra of the system are considered vertical then  $\text{RFe}_3(\text{BO}_3)_4$  ferroborate crystal structure can be looked at as a sequence of horizontal layers. The distance between the nearest equivalent layers is one third of the vertical period of the structure  $c$ , with the latter being the height of the unit cell of  $\text{RFe}_3(\text{BO}_3)_4$  system in hexagonal crystallographic coordinates. The hexagonal unit cell then comprises three chemical units ( $Z = 3$ ), i.e. three equivalent  $\text{R}^{3+}$  ions and correspondingly nine  $\text{Fe}^{3+}$  ions.

When considering the peculiarities of the crystal structure of the system under consideration we would refer to the advanced recently appeared data [8] fully devoted to the detailed gadolinium ferroborate structure determination. Due to the Ref. [8], the  $\text{GdFe}_3(\text{BO}_3)_4$  system space group transforms at the structural phase transition temperature  $T_C$  in the manner  $R32 \geq P3_121$ , with the primitive unit cell volume of the system being tripled and the hexagonal unit cell becoming primitive. As far as the symmetry aspects of the structural phase transition are concerned, one should firstly mention that at  $T_C$  the system loses a distinct number of translation transformations, which means that its Bravais lattice is changed. Then all 3 proper rotation axes disappear, from the six previously existed  $3_1$  screw axes only three survive. A great number of 2 rotation axes (in correspondence with the new space group rules) disappears. Meanwhile, the crystal class of the system (characterizing its macro-symmetry)  $D_3$  which is of great importance stays the same.

As a result of the structural phase transition the number of magnetoactive  $\text{Fe}^{3+}$  ions imbedded in the primitive unit cell counts nine, although they now form two different subsystems—  $\text{Fe}^{3+}$  (1) ions (with multiplicity 3) and  $\text{Fe}^{3+}$  (2) ions (occupying general position with multiplicity 6). For the determination of independent magnetic modes to appear in the system at magnetic phase transition (we will exclude from our consideration for a while rare earth ions) and in correspondence with the space group representations theory we will take for treating low temperature ( $T < T_C$ ) crystal symmetry group the main  $3_1$  screw axis transformation, the 2 proper rotation transformation (performing through the 2 proper axis lying in the base of the unit cell and passing through the  $3_1$  screw axis) and basic  $T_a$  and  $T_b$  translations (performing along  $a$  and  $b$  edges of the base) as generic transformations. Actually the third power of the  $3_1$  screw axis transformation will be equivalent to  $T_c$  translation transformation. The  $3_1$  screw axis transformations due to the other two  $3_1$  screw axes can be easily shown to be equivalent to the combination of the main screw axis transformation and the consecutive translation  $T_a$  or  $T_{a+b}$ , respectively. As follows from [9] magnetic phase transition does not change basal translations of the system, then from magnetic symmetry viewpoint translations  $T_a$  and  $T_b$  will be equivalent to identity transformation  $E$ . As a matter of fact for active irreducible representation (responsible for the magnetic transformation at  $T_N$ ) construction it is suffice to consider an auxiliary (limited) symmetry group  $G'_{32}$  with  $3_1$  and 2 transformations as its generators. Antiferromagnetic ordering to occur in the system at  $T_N$  as was already mentioned [9] leads to doubling of the elementary unit cell along  $c$ -axis. Just for this reason the  $G'_{32}$  group will comprise 12 elements—screw axis transformations  $3_1^1, 3_1^2, 3_1^3, 3_1^4, 3_1^5, 3_1^6$  and proper rotations  $2_{a+b}(0), 2_{a+b}(1/2), 2_a(1/3), 2_a(5/6), 2_b(1/6), 2_b(2/3)$ , where the lower index means the direction of the corresponding rotation axis and the number in brackets means the height of the axis inside the unit cell. We will enumerate 18  $\text{Fe}^{3+}$  ions imbedded in the doubled  $\text{GdFe}_3(\text{BO}_3)_4$  cell in correspondence with their position in regard to the nearest  $3_1$  axis. The main  $3_1 \equiv 3_1^1$  axis permutes the spins  $\text{S}_2(0), \text{S}_3(1/3), \text{S}_1(2/3), \text{S}_2(1), \text{S}_3(4/3), \text{S}_1(5/3)$  (the lower index corresponds to the number of spin in the horizontal layer and the one in brackets—the height of the layer inside the elementary cell). The axes  $3_1^{\text{II}}$  and  $3_1^{\text{III}}$  permute the spins  $\text{S}_1(0), \text{S}_2(1/3), \text{S}_3(2/3), \text{S}_1(1), \text{S}_2(4/3), \text{S}_3(5/3)$  and  $\text{S}_3(0), \text{S}_1(1/3), \text{S}_2(2/3), \text{S}_3(1), \text{S}_1(4/3), \text{S}_2(5/3)$  correspondingly. Symmetry adapted linear combinations of all 18 spins mentioned above describe independent magnetic modes and form bases of irreducible representations of  $G'_{32}$  group (whose number is 6). As an order parameter in exchange approximation we would get either one of four one-dimensional representations, corresponding to collinear magnetic orderings, or one of two two-dimensional representations, describing exchange non-collinear magnetic structure. One can, for example, easily show with the use of group representations theory that 6

spins corresponding to  $3_1^{\text{I}}$  axis form bases of the following irreducible representation

$$\begin{aligned} \mathbf{F}^{(+)} &= \mathbf{S}_2(0) + \mathbf{S}_3(1/3) + \mathbf{S}_1(2/3) + \mathbf{S}_2(1) + \mathbf{S}_3(4/3) + \mathbf{S}_1(5/3), \\ \mathbf{L}^{(-)} &= \mathbf{S}_2(0) - \mathbf{S}_3(1/3) + \mathbf{S}_1(2/3) - \mathbf{S}_2(1) + \mathbf{S}_3(4/3) - \mathbf{S}_1(5/3), \\ &\left\{ \begin{aligned} \mathbf{B}_1^{(+)} &= \sqrt{3}[\mathbf{S}_2(0) + \mathbf{S}_2(1) - \mathbf{S}_3(1/3) - \mathbf{S}_3(4/3)] \\ \mathbf{B}_2^{(+)} &= \mathbf{S}_2(0) + \mathbf{S}_2(1) + \mathbf{S}_3(1/3) + \mathbf{S}_3(4/3) \\ &\quad - 2[\mathbf{S}_1(2/3) + \mathbf{S}_1(5/3)] \end{aligned} \right\}, \\ &\left\{ \begin{aligned} \mathbf{B}_1^{(-)} &= \sqrt{3}[\mathbf{S}_2(0) - \mathbf{S}_2(1) + \mathbf{S}_3(1/3) - \mathbf{S}_3(4/3)] \\ \mathbf{B}_2^{(-)} &= \mathbf{S}_2(0) - \mathbf{S}_2(1) - \mathbf{S}_3(1/3) + \mathbf{S}_3(4/3) \\ &\quad - 2[\mathbf{S}_1(2/3) - \mathbf{S}_1(5/3)] \end{aligned} \right\}. \end{aligned}$$

For 12 other spins (corresponding to  $3_1^{\text{II}}$  and  $3_1^{\text{III}}$  axes) we similarly get bases of four one-dimensional and four different two-dimensional representations. We will be interested in only one of them, namely, one-dimensional combination

$$\begin{aligned} \mathbf{L}^{(-)} &= \mathbf{S}_1(0) + \mathbf{S}_3(0) - \mathbf{S}_2(1/3) - \mathbf{S}_1(1/3) + \mathbf{S}_3(2/3) \\ &\quad + \mathbf{S}_2(2/3) - \mathbf{S}_1(1) - \mathbf{S}_3(1) + \mathbf{S}_2(4/3) + \mathbf{S}_1(4/3) \\ &\quad - \mathbf{S}_3(5/3) - \mathbf{S}_2(5/3). \end{aligned}$$

As follows from Ref. [9], the collinear antiferromagnetic ordering to occur in our system at  $T_N$  will be described by the combined antiferromagnetic vector  $\mathbf{L} = \mathbf{L}^{(-)} + \mathbf{L}'^{(-)}$

With the help of the Table 1 of our previous work [10] we easily get magnetoelectric

$$\begin{aligned} \Phi_{\text{ME}} &= \beta_1 \{ P_X(L_X^2 - L_Y^2) - 2P_Y L_X L_Y \} \\ &\quad + \beta_2 L_Z(P_X L_Y - P_Y L_X) \\ &\quad + \beta_3 P_Z L_Z(L_X^3 - 3L_X L_Y^2) \end{aligned}$$

and magnetoelastic

$$\begin{aligned} \Delta\Phi_{\text{Mel}} &= \gamma_1^1 u_{ZZ} L_Z^2 + \gamma_1^2 u_{ZZ}(L_X^2 + L_Y^2) \\ &\quad + \gamma_2^1(u_{XX} + u_{YY})L_Z^2 + \gamma_2^2(u_{XX} + u_{YY})(L_X^2 + L_Y^2) \\ &\quad + \gamma_3[(u_{XX} - u_{YY})(L_X^2 - L_Y^2) + 4u_{XY}L_X L_Y] \\ &\quad + \gamma_4[u_{YZ}(L_X^2 - L_Y^2) + 2u_{XZ}L_X L_Y] \\ &\quad + \gamma_5[(u_{XX} - u_{YY})L_Y L_Z + 2u_{XY}L_X L_Z] \\ &\quad + \gamma_6[u_{YZ}L_Y L_Z + u_{XZ}L_X L_Z] \end{aligned}$$

contributions. Due to the results of Ref. [10] the expressions for magnetoelectric and magnetoelastic interactions written above can be immediately shown to interpret the results of our experiment.

## Acknowledgements

This work is supported by RFBR Grant 04-02-16592. Authors thank A.N. Vasil'ev and M.N. Popova for helpful discussions.

**References**

- [1] A.M. Kalashnikova, V.V. Pavlov, R.V. Pisarev, L.N. Bezmaternykh, M. Bayer, Th. Rasing, JETP Lett. 80 (2004) 293.
- [2] J.A. Campa, C. Cascales, E. Gutierrez-Puebla, M.A. Monge, I. Rasines, C. Ruiz-Valero, Chem. Mater. 9 (1997) 237.
- [3] Y. Hinatsu, Y. Doi, K. Ito, M. Wakeshima, A. Alemi, J. Solid State Chem. 172 (2003) 438.
- [4] A.D. Balaev, L.N. Bezmaternykh, I.A. Gudim, V.L. Temerov, S.G. Ovchinnikov, S.A. Kharlamova, JMMM 258–259 (2003) 532.
- [5] R.Z. Levitin<sup>†</sup>, E.A. Popova, R.M. Chtsherbov, A.N. Vasiliev, M.N. Popova, E.P. Chukalina, S.A. Klimin, P.H.M. van Loosdrecht, D. Fausti, L.N. Bezmaternykh, JETP Lett. 79 (2004) 429.
- [6] A.N. Vasil'ev, private communications.
- [7] A.K. Zvezdin, S.S. Krotov, A.M. Kadomtseva, G.P. Vorob'ev, Yu.F. Popov, A.P. Pyatakov, L.N. Bezmaternykh, E.A. Popova, JETP Lett. 81 (2005) 272.
- [8] S.A. Klimin, D. Fausti, A. Meetsma, L.N. Bezmaternykh, P.H.M. van Loosdrecht, T.T.M. Palstra, Acta Crystallogr. B 61 (2005) 481.
- [9] A.I. Pankrats, G.A. Petrakovskii, L.N. Bezmaternykh, O.A. Bayukov, JETP 99 (2004) 766.
- [10] A.M. Kadomtseva, Yu.F. Popov, S.S. Krotov, G.P. Vorob'ev, E.A. Popova, A.K. Zvezdin, L.N. Bezmaternykh, Low Temp. Phys. 31 (2005) 757.